8

Detailed Flow Structure around a Thermohaline Front at the Mouth of Ise Bay, Japan

Tetsuo Yanagi, Xinyu Guo, Takashi Ishimaru and Toshiro Saino

Abstract

Detailed flow structure around a thermohaline front at the mouth of Ise Bay, Japan was observed with use of ADCP (Acoustic Doppler Current Profiler). The surface water converges at the transition zone between cold coastal water and warm off-shore water, sinks there and diverges like a skirt in the lower layer below the transition zone. The maximum surface convergence and sinking velocity are 5.0 x 10^{-4} s^{-1} and 0.25 cm s^{-1}, respectively.

1. Introduction

Quasi-steady thermohaline fronts develop on the shelf areas of the northwestern Pacific Ocean in winter [e.g. Nagashima and Okazaki, 1979, Yanagi, 1980, Lie, 1985]. The generation and maintenance mechanisms of such fronts have been investigated mainly with use of numerical models by Endoh [1977], Harashima and Oonishi [1981], and Akitomo et al. [1990]. From their results, the front is generated in a transition zone between cold and fresh coastal water and warm and saline oceanic water due to surface cooling and fresh water inflow from land but there is little density difference between both sides of the front because the salinity difference compensates the temperature difference. The front exists at nearly the same position from late autumn to early spring and plays an important role on the material transport [Yoshioka, 1988, Yanagi et al., 1989].

A remarkable thermohaline front is observed at the mouth of Ise Bay in winter and the distributions of water temperature and salinity around this front and their seasonal variations have been investigated [Sekine et al., 1992, Yanagi et al., 1995]. The detailed flow structure around this front, however, is not yet known. We report here the three-dimensional detailed flow structure around a thermohaline front at the mouth of Ise Bay, Japan.

2. Field observation

The field observations were carried out at the mouth of Ise Bay (Figure 1) by R.V. *Tansei-Maru* of the Ocean Research Institute, University of Tokyo, on 11 and 12 February 1995. The vertical profiles of water temperature and salinity were observed with use of CTD (Neil Brown Mark III B) at 9 stations from Sta. IF-2 to Sta. IF-10 shown in Figure 1 during 14:58 through 17:33 on 11 February 1995. The distance between successive observation stations is about 900 m. The horizontal distributions of water temperature at surface (1.0 m depth) and velocity at the depth of 3.5 m, 5.5 m, 7.5 m, 9.5 m, 11.5 m, 13.5 m, 15.5 m, 17.5 m and 19.5 m were

Buoyancy Effects on Coastal and Estuarine Dynamics
Coastal and Estuarine Studies Volume 53, Pages 97-106

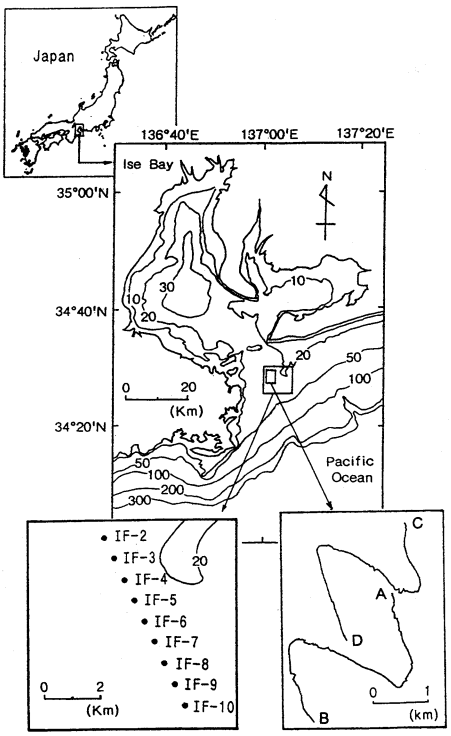

Figure 1. Ise Bay. Numbers show the depth in meter.

observed continuously along the observation lines from A to B (see Figure 1) during 10:56 to 11:44 on 12 February and from C to D during 12:28 to 13:08 on 12 February with use of a thermistor and an ADCP (RD Instruments, 300 kHz). Averaged water depth along A-B and C-D lines is about 23 m. Water temperature and velocity were measured at 15 seconds intervals, which corresponds to a 15 m interval for R.V. *Tansei-Maru* steaming at about 2 kt. Raw data were filtered with use of a box filter (60 m in horizontal length and 4 m in vertical length).

3. Results

Figure 2 is a NOAA 12 infra-red image, collected at 8:00 JMT on 11 February 1995, which shows the position of the thermohaline front at the mouth of Ise Bay. The thermohaline front, represented by a discontinuity line between cooler coastal water and warmer offshore water, runs in a northeast to southwest direction at the mouth of Ise Bay. Due to cooling through the sea surface in winter, water at the mouth of Ise Bay with moderate salinity becomes the heaviest and sinks there. The colder coastal water cannot become heavy enough to sink due to the fresh water inflow from land. Oceanic saline water also cannot become heavy enough to sink because of the mixing with warm Kuroshio water. The thermohaline front exists here from late autumn to early spring with short-term variation of the period of 10 to 15 days [Sekine et al., 1992].

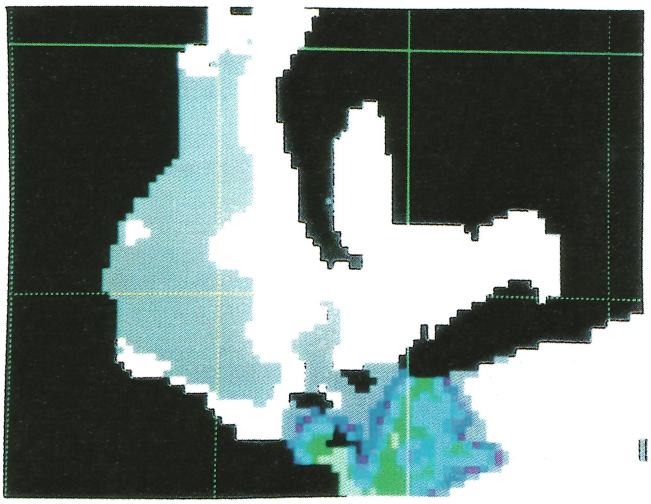

Figure 2. NOAA 12 infra red image collected at 8:00 JMT on 11 February 1995.

The observed vertical distributions of water temperature and salinity across this front are shown in Figure 3. The horizontal gradients of water temperature and salinity up to 3.0°C km-1 and 1.0 psu km-1, respectively, are observed in the surface layer.

On the other hand, the density gradient does not exist across the transition zone as seen in water temperature and salinity distributions. It appears that the surface water converges at the transition zone (near Sta. IF-5 in this case), sinks there and diverges like a skirt in the lower layer as shown in Figure 3. Such distribution patterns have been observed at a thermohaline front in the Kii Channel [Yoshioka, 1984] and at the mouth of Tokyo Bay [Yanagi et al., 1989].

The northward flood tidal current was dominant at the observation period along A-B and C-D lines on 12 February 1995 and the frontal structure was considered to be advected in a frozen manner by this tidal current. Therefore we first estimated the barotropic tidal current field at the observation period on 12 February. The horizontal distributions of vertically averaged velocity along A-B and C-D lines are shown in Figure 4. The averaged northward current is predominant at all observation points. The speed along the C-D line is larger than that along the A-B line. We assume that little alteration in vertical and horizontal frontal structure took place in a general northward barotropic tidal current field during our observation period of 48 minutes (A-B line) and 40 minutes (C-D line), respectively. Hence we shift the position of the observation points along A-B and C-D lines to the positions at the beginning of our field observation, that is, at 10:56 on 12 February along the A-B line and at 12:28 on 12 February along the C-D line, respectively; each observation point was moved to upstream direction by the distance calculated by multiplying the vertically averaged velocity at each point (shown in Figure 4) with the time difference between the beginning time and the observation time. The reconstructed horizontal distributions of surface (1 m depth) water temperature at the beginning of the observation are shown in Figure 5. Temperature values are objectively interpolated at each grid (100 m mesh size) with use of a hyperbolic function [Yanagi and Igawa, 1992] from the observed data along A-B and C-D lines. The maximum horizontal gradient of water temperature is 2.5°C / 200 m.

The horizontal distributions of anomaly velocity at each depth from the vertically averaged velocity are shown in Figure 6. They are also objectively interpolated in the same manner as in Figure 5. The southward flow is dominant in the upper layer and the northward flow in the lower layer. The colder coastal water and warmer oceanic water in the surface layer

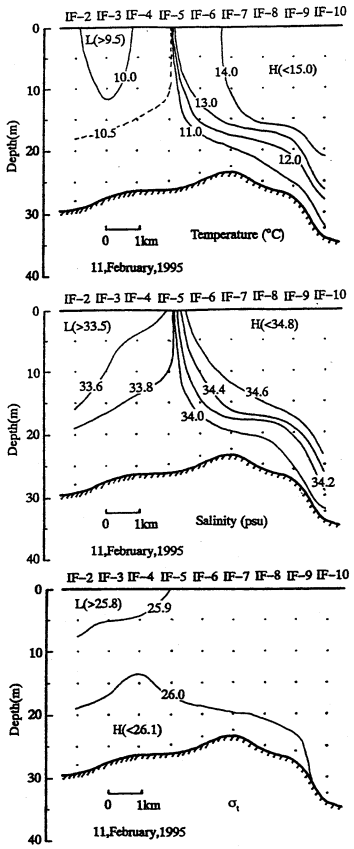

Figure 3. Vertical distributions of water temperature, salinity and sigma t across the thermohaline front at the mouth of Ise Bay.

seem to converge to the frontal zone. The water at the middle layer (11.5 m depth) stagnates. On the other hand, the colder coastal water and warmer oceanic water at the depth of 17.5 m seem to diverge from the transition zone.

The horizontal distributions of convergence and divergence Q, defined by Eq. (1), at each depth are calculated as.

$$Q = \frac{\partial u}{\partial x} + \frac{\partial v}{\partial y} \tag{1}$$

Here u denotes the eastward velocity and v the northward velocity. The relative error of observed velocity by ADCP is +/- 1 cm s^{-1} and that of positioning every 15 m by GPS (Global Positioning System) +/- 1 m because the sea surface was very calm during the observation. Therefore the accuracy of calculated Q is +/- 4 x 10^{-5} s^{-1} which is obtained by the relative accuracy of current / that of positioning.

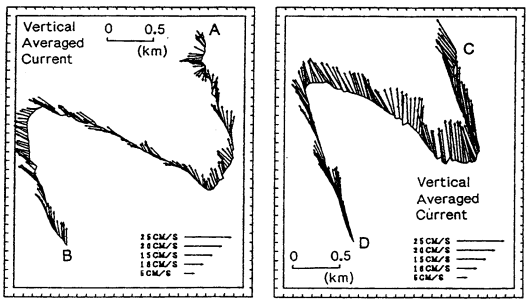

Figure 4. Vertically averaged currents along A-B and C-D lines.

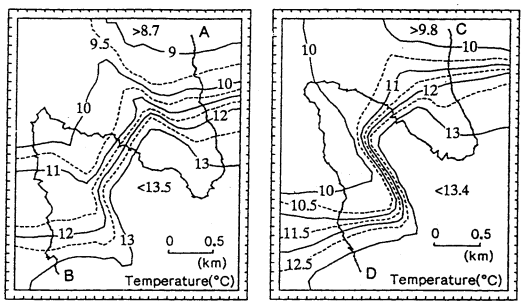

Figure 5. Horizontal distribution of water temperature (1 m depth) along A-B and C-D lines.

The evaluated horizontal distributions of Q at each depth are shown in Figure 7. The surface convergence with the value of -5.0×10^{-4} s^{-1} is seen just at the transition zone of water temperature shown in Figure 5 and the large divergence of 5.0×10^{-4} s^{-1} is seen at the depth of 17.5 m just below the surface convergence zone. The surface divergence zone exists next to the convergence zone at each depth of this observation area. The observed divergence or convergence is one-order of magnitude larger than those observed in the coastal sea [e.g. Akamatsu, 1975] or open ocean [e.g. Molinari and Kirwan, 1975] except at the frontal region [e.g. Tomosada et al., 1986]. The vertical velocity is estimated on the basis of the continuity equation and the Q shown in Figure 7. It is assumed that the vertical velocity W (positive upward) and horizontal divergence Q at the sea surface are 0.

It is shown as,

$$W_{z=3.5m} = \frac{1}{2} \; Q_{z=3.5m} \; x \; 350cm \tag{2}$$

Vertical velocities at the each depth are estimated successively in the same manner and shown as,

Figure 6. Horizontal distributions of anomaly velocity from the vertically averaged one along A-B and C-D lines.

$$W_{z=5.5m} = \frac{1}{2}\left(Q_{z=3.5m} + Q_{z=5.5m}\right) x\ 200\ cm + W_{z=3.5m} \tag{3}$$

$$W_{z=11.5m} = \frac{1}{2}\left(Q_{z=9.5m} + Q_{z=11.5m}\right) x\ 200cm + W_{z=9.5m} \tag{4}$$

$$W_{z=17.5m} = \frac{1}{2}\left(Q_{z=15.5m} + Q_{z=17.5m}\right) x\ 200cm + W_{z=15.5m} \tag{5}$$

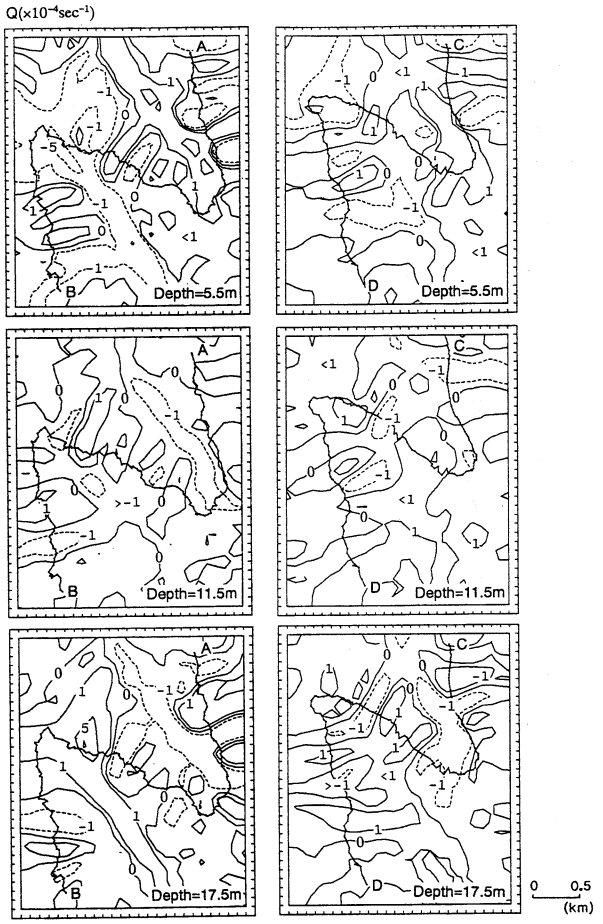

Figure 7. Horizontal distributions of divergence (+) and convergence (-) at three depths.

The accuracy of estimated vertical velocity is +/- 0.008 cm s^{-1} on the basis of the accuracy of Q. The estimated horizontal distributions of vertical velocity at each depth are shown in Figure 8. The large downward velocity is seen at the depth of 11.5 m and it attains 0.25 cm s^{-1}.

Based on Figure 3, Figure 6 and Figure 8, the flow structure around the thermohaline front can be delineated. The surface coastal water and the surface oceanic water are advected to the thermohaline front at the speed of about 10 cm s-1. The downward velocity of 0.1 cm s^{-1} is seen at the surface convergence zone. The maximum downward current appears at the middle layer just below the surface convergence zone and it is about 0.25 cm s^{-1}. Interestingly, an upward current coexists with the downward current at the depth of 11.5 m. This may indicate the existence of strong gravitational convection due to sea surface cooling at the transition zone which was suggested by Akitomo et al. [1990]. Below the mid-depth mixing layer, the mixed water diverges to both sides of the front with the speed of about 10 cm s^{-1}. This estimation of vertical velocity, although just a snapshot at the frontal region, is the first case where the directly observed current data were utilized to reconstruct a three-dimensional flow field around a coastal front.

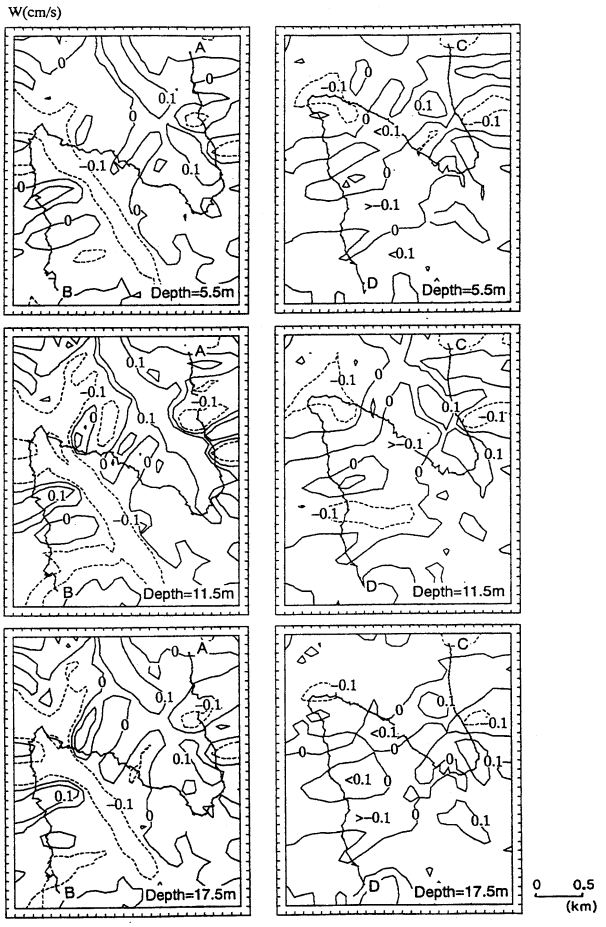

Figure 8. Horizontal distribution of upward velocity (+) an downward one (-) at three depths

The magnitude of vertical velocity obtained here is about twice as that estimated theoretically for the front driven by the cabling effect [Horne et al., 1978], and nearly the same as that estimated by diagnostic model calculation using the observed density distribution data at a thermohaline front at the mouth of Tokyo Bay [Yanagi et al., 1989]. The calculated vertical velocity in the mid-depth is not shown directly in Akitomo et al. [1990] but we can guess that their calculated vertical velocity is nearly the same as ours because they obtained nearly the same surface convergence values in their numerical model as ours. However, the calculated values mentioned above are all based on the vertical two dimensional analysis though our present observed current field shows the dominant three-dimensional structure. We have to carry out a three-dimensional numerical experiment in the near future in order to investigate the dynamics of three-dimensional current field around a thermohaline front.

4. Discussions

The material transport from the coastal sea to the open sea plays an important role in global material cycling [IGBP Report No. 25, 1993]. One of the main goals of IGBP/LOICZ (International Geosphere/Biosphere Programme, Land-Ocean Interaction in Coastal Zone) Project is to quantitatively estimate the material transport from the coastal sea to the open sea. To attain that goal, it is essential to evaluate the role of coastal fronts on the material transport, because there are various types of oceanic fronts in the coastal sea [Yanagi, 1987]. The material flux itself can be estimated simply by multiplying the material concentration and the current speed. It must be stressed that the variables required for this calculation are the material concentrations and the current speed averaged on relevant time and spatial scales because the temporal and spatial variations of coastal front is very large and such variability plays important role in the material transport [e.g. Akitomo, 1988]. The instantaneous three-dimensional flow structure around a thermohaline front shown here is the first step to clarify the time and spatial scales of material transport dynamics in the coastal sea.

The coastal fronts also play important roles in the coastal ecosystem [e.g. Kiorboe et al., 1988]. It is well known that coastal fronts are good spawning grounds of many fish species [Boucher et al., 1987], because phytoplankton and zooplankton are accumulated by the surface converging currents and serve as food necessary for the survival of fish larvae [Uye et al., 1992]. Given the maximum downward flow speed of 0.25 cm s^{-1}, larvae entrained into the downwelling stream will be transported to the bottom (- 23 m) in about 2.5 hours. In this case, only the larvae whose swimming speed exceeds the water movement speed may survive. Hence the instantaneous flow field should be taken into account when we consider the phenomena of relevant time and spatial scales such as biological processes in ecosystem dynamics around coastal fronts.

Acknowledgments. We thank to officers and crews of R.V. *Tansei-Maru* for their help in the field observation. This study was partially supported by the fund defrayed from the Ministry of Education, Science and Culture, Japan.

References

Akamatsu, H., On the oceanographic structure at the frontal zone in Japan Sea (I), *Umi to Sora, 50,* 123-136, 1975. (in Japanese).

Akitomo, K., A numerical study of a shallow sea front generated by the buoyancy flux: water exchange caused by fluctuation of the front, *J. Oceanogr. Soc. Japan, 44,* 171-188, 1988.

Akitomo, K., N. Imasato, and T. Awaji, A numerical study of a shallow sea front generated by buoyancy flux: generation mechanism, *J. Physical Oceanogr., 20,* 172-189, 1990.

Boucher, J., F. Ibanez, and L. Prieur, Daily and seasonal variations in the spatial distribution of zooplankton populations in relation to the physical structure in the Ligurial Sea Front, *J. Mar. Res., 45,* 133-173, 1987.

Endoh, M., Formation of thermohaline front by cooling of the sea surface and inflow of the fresh water, *J. Oceanogr. Soc. Japan, 33,* 6-15, 1977.

Harashima, A., and Y. Oonishi, The Coriolis effect against frontogenesis in steady buoyancy-driven circulation, *J. Oceanogr. Soc. Japan, 37,* 49-59, 1981.

Horne, E.P.W., M.J. Bowman, and A. Okubo, Crossfrontal mixing and cabling, in *Oceanic Fronts in Coastal Processes,* edited by M.J. Bowman and W.E. Esaias, pp. 105-113, Springer-Verlag, New York, 1978.

IGBP Report No. 25, 50 p, 1993.

Kiorboe, T., P. Munk, K. Richardson, V. Christensen, and H. Paulsen, Plankton dynamics and larval herring growth, drift and survival in a frontal area, *Mar. Ecol. Prog. Ser., 44,* 205-219, 1988.

Lie, H.J., Wintertime temperature-salinity characteristics in the south-eastern Hwanghae (Yellow Sea), *J. Oceanogr. Soc. Japan, 41,* 291-298, 1985.

Molinari, A., and A.D. Kirwan, Calculations of differential kinetic properties from Lagranjian observations in the western Caribbean Sea, *J. Physical Oceanogr., 5,* 483-491, 1975.

Nagashima, H., and M. Okazaki, Currents and oceanic condition at Tokyo Bay in winter, *Bulletin on Coastal Oceanography, 16,* 76-86, 1979 (in Japanese).

Sekine, Y., S. Kawamata, and Y. Satoh, Observation of coastal fronts in Ise Bay in early winter, *Bulletin on Coastal Oceanography, 29,* 190 - 196, 1992 (in Japanese with English abstract and captions).

Tomosada, A., K. Segawa, and K. Kuroda, Closely-spaced observations across the Kuroshio front south of the Shionomisaki, *Bull. Tokai Reg. Fish. Res. Lab., 120,* 11-25,1986 (in Japanese).

Uye, S., T. Yamaoka, and T. Fujisawa, Are tidal fronts good recruitment areas for herbivorous copepods?. *Fisheries Oceanography, 1,* 216-226, 1992.

Yanagi, T., A coastal front in the Sea of Iyo, *J. Oceanogr. Soc. Japan, 35,* 253-260, 1980.

Yanagi, T., Classification of "Siome", streaks and fronts, *J. Oceanogr. Soc. Japan, 43,* 149-158, 1987.

Yanagi, T., and T. Koike, Seasonal variation in thermohaline and tidal fronts, Seto Inland Sea, Japan, *Cont. Shelf Res., 7,* 149-160, 1987.

Yanagi, T., A. Isobe, T. Saino, and T. Ishimaru, Thermohaline front at the mouth of Tokyo Bay, *Cont. Shelf Res., 9,* 77-91, 1989.

Yanagi, T., O. Matsuda, S. Tanabe and S. Uye (1992) Interdisciplinary study on the tidal front in the Bungo Channel, Japan, in *Dynamics and Exchanges in Estuaries and the Coastal Zone,* edited by D. Prandle, pp. 617-630, AGU, Washington, DC, 1992.

Yanagi, T., and S. Igawa (1992) Diagnostic numerical model of residual flow in the coastal sea, *Bulletin on Coastal Oceanogr., 30,* 108-115,1992, (in Japanese).

Yanagi, T., X. Guo, T. Saino, and T. Ishimaru, Thermohaline front at the mouth of Ise Bay in winter, 1995, (to be submitted).

Yoshioka, H., Oceanic fronts in the coastal sea, *Bulletin on Coastal Oceanography, 21,* 110-117, 1984, (in Japanese).

Yoshioka, H., The coastal front in the Kii Channel in winter, *Umi to Sora., 64,* 79-111, 1988.